

Journal Club

“The story on the short-range
transition operator for neutrinoless
double-beta decay”

Sep.18, 2023

Nuclear Theory

[Submitted on 7 Aug 2023]

A relativistic model-free prediction for neutrinoless double beta decay at leading order

Y. L. Yang, P. W. Zhao

Starting from a manifestly Lorentz-invariant chiral Lagrangian, we present a model-free prediction for the transition amplitude of the process $nn \rightarrow ppe^-e^-$ induced by light Majorana neutrinos, which is a key process of the neutrinoless double beta decay ($0\nu\beta\beta$) in heavy nuclei employed in large-scale searches. Contrary to the nonrelativistic case, we show that the transition amplitude can be renormalized at leading order without any uncertain contact operators. The predicted amplitude defines a stringent benchmark for the previous estimation with model-dependent inputs, and greatly reduces the uncertainty of $0\nu\beta\beta$ transition operator in the calculations of nuclear matrix elements. Generalizations of the present framework could also help to address the uncertainties in $0\nu\beta\beta$ decay induced by other mechanisms. In addition, the present work motivates a relativistic ab initio calculation of $0\nu\beta\beta$ decay in light and medium-mass nuclei.

Comments: 6 pages, 4 figures. Comments and suggestions are welcome

Subjects: **Nuclear Theory (nucl-th)**; High Energy Physics - Lattice (hep-lat); High Energy Physics - Phenomenology (hep-ph)

Cite as: [arXiv:2308.03356](https://arxiv.org/abs/2308.03356) [nucl-th]

(or [arXiv:2308.03356v1](https://arxiv.org/abs/2308.03356v1) [nucl-th] for this version)

<https://doi.org/10.48550/arXiv.2308.03356> 

Introduction.—Neutrinoless double beta decay ($0\nu\beta\beta$) is a second-order weak process, in which a nucleus decays to its neighboring nucleus by turning two neutrons to two protons, emitting two electrons but no corresponding antineutrinos [1]. Its observation would provide direct evidence of lepton number violation beyond the standard model, prove the Majorana nature of neutrinos [2], constrain the neutrino mass scale and hierarchy [3], and shed light on the matter-antimatter asymmetry in the Universe [4]. Therefore, it becomes one of the top priorities in the field of nuclear and particle physics, and invigorates worldwide experiments either activate or planned [5–12] (for a recent review, see Ref. [13]).

Nuclear matrix element, which encodes the impact of the nuclear structure on the decay half-life, is crucial to interpreting the experimental limits and even more potential future discoveries. Within the standard picture of $0\nu\beta\beta$, which involves the long-range light neutrino exchange [14], a minimal extension of the standard model, current knowledge of the nuclear matrix element is not satisfactory [15], as various nuclear models lead to discrepancies as large as a factor around 3.

Chiral effective field theory (EFT) [16, 17] plays an important role in addressing such uncertainties. It can provide the nuclear Hamiltonian and weak currents in a consistent and systematically improvable manner [18–20]. Based on chiral EFT, the issue of g_A quenching in single β decays [21] was resolved as a combination of two-nucleon weak currents and strong nuclear correlations [22, 23]. The chiral-EFT-based $0\nu\beta\beta$ transition operators under various sources of lepton number violation [24–30], as well as their impacts on the nuclear matrix elements have been extensively studied in the literature [31–36]. In addition, *ab initio* calculations of nuclear matrix elements using a chiral Hamiltonian are available recently [37–40].

In the context of the standard light Majorana neutrino-exchange mechanism [14], Cirigliano *et al.* showed that a chiral EFT description of $0\nu\beta\beta$ decay, already at leading order (LO), requires a contact operator to ensure

renormalizability [27, 28]. The size of this contact term should be determined in principle by matching to first-principle gauge field theory calculations, which however are not yet available currently (see Refs. [41–49] for related progress). This unknown contact term, thus, leads to an additional source of uncertainty for the nuclear matrix elements besides the nuclear-structure ones.

Cirigliano *et al.* [29, 30] first estimated the contact term by computing the $nn \rightarrow ppe^-e^-$ transition amplitude in an integral representation, i.e., a momentum integral of the neutrino propagator times the generalized forward Compton scattering amplitude. The underlying model introduces, in the intermediate-momentum region, model-dependent inputs from elastic intermediate states in analogy to the Cottingham formula [50]. Therefore, a model-free determination of the contact term is still missing, in the absence of costly calculations based on lattice gauge theory.

In this Letter, we present a model-free prediction of the $nn \rightarrow ppe^-e^-$ amplitude by developing a relativistic framework based on chiral EFT. We show that the transition amplitude can be renormalized at LO without the vague contact term in the relativistic framework starting from a manifestly Lorentz-invariant chiral Lagrangian. Matching to our results will allow one to stringently determine the contact term needed in nonrelativistic nuclear-structure calculations, and to greatly reduce the corresponding uncertainty in the calculations of nuclear matrix elements for $0\nu\beta\beta$ decay. It also paves the way to relativistic *ab initio* calculations of $0\nu\beta\beta$ decay rates in light and medium-mass nuclei.

Relativistic framework.—We start from a manifestly Lorentz-invariant effective Lagrangian relevant at the leading order of chiral EFT [19],

$$\begin{aligned} \mathcal{L}_{\Delta L=0} = & \frac{f_\pi^2}{4} \text{tr}[u_\mu u^\mu + m_\pi^2(uu + u^\dagger u^\dagger)] \\ & + \bar{\Psi}(i\gamma^\mu D_\mu - M + \frac{g_A}{2}\gamma^\mu\gamma_5 u_\mu)\Psi - \sum_\alpha \frac{C_\alpha}{2}(\bar{\Psi}\Gamma_\alpha\Psi)^2, \end{aligned} \quad (1)$$

这篇论文是探讨

无中微子双贝塔衰变中“短程”跃迁算符的贡献。

这故事还得从2018年说起。

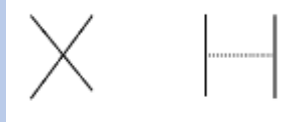
New Leading Contribution to Neutrinoless Double- β Decay

Vincenzo Cirigliano, Wouter Dekens, Jordy de Vries, Michael L. Graesser, Emanuele Mereghetti, Saori Pastore, and Ubirajara van Kolck

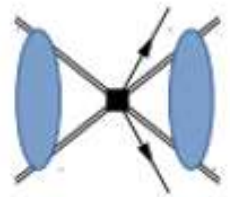
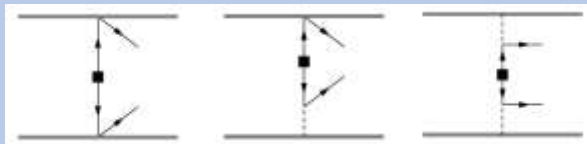
Phys. Rev. Lett. **120**, 202001 – Published 16 May 2018

Physics See Synopsis: [A Missing Piece in the Neutrinoless Beta-Decay Puzzle](#)

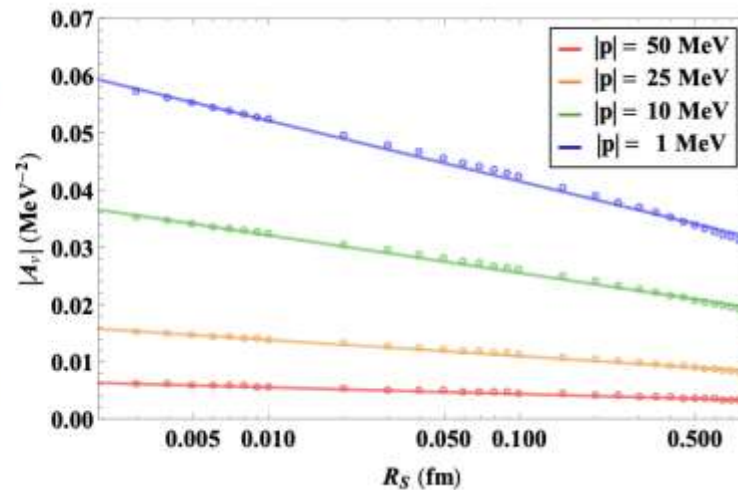
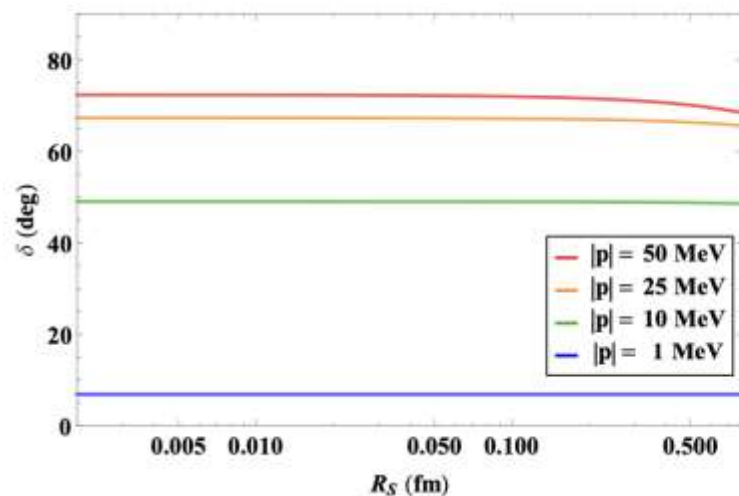
Nuclear force



Transition operator



CT



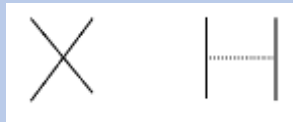
New Leading Contribution to Neutrinoless Double- β Decay

Vincenzo Cirigliano, Wouter Dekens, Jordy de Vries, Michael L. Graesser, Emanuele Mereghetti, Saori Pastore, and Ubirajara van Kolck

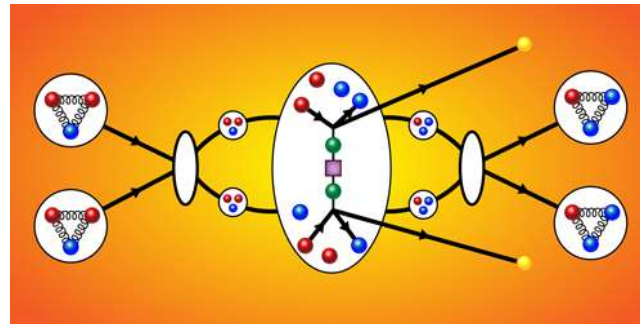
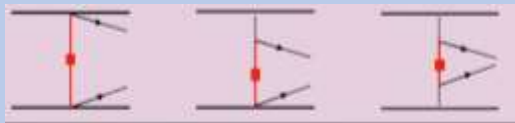
Phys. Rev. Lett. **120**, 202001 – Published 16 May 2018

Physics See Synopsis: [A Missing Piece in the Neutrinoless Beta-Decay Puzzle](#)

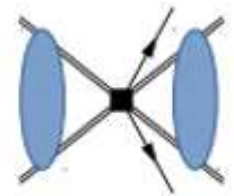
Nuclear force



Transition operator



divergent



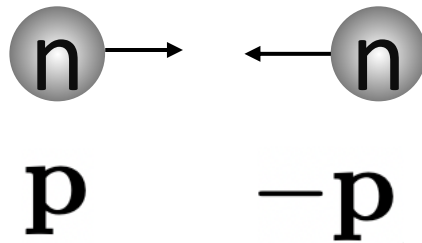
CT

Cirigliano and collaborators show that reliable amplitude calculations must include a contribution due to interactions acting on short ranges (less than 1 femtometer). Previous studies had only included longer-range contributions acting on scales up to a few femtometers. The short-range contribution generates a transition amplitude that might be as large as the one calculated based on the long-range component only. The short- and long-range components could add up to make the neutrinoless decay more likely, or they could partly cancel out to make it less likely. More work is needed to determine the sign and magnitude of the short-range component. The authors' preliminary estimates, however, indicate that it could significantly affect the neutrino mass properties derived from double-beta-decay experiments.

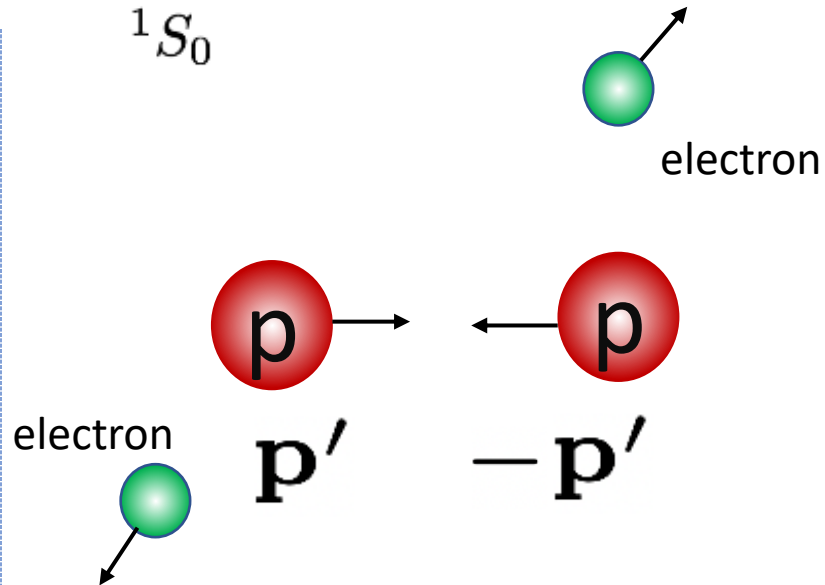
<https://physics.aps.org/articles/v11/s58>

Considering the process: $2n$ decay into $2p + 2e$

$$n(\mathbf{p})n(-\mathbf{p}) \xrightarrow{{}^1\hat{S}_0} p(\mathbf{p}')p(-\mathbf{p}')e(\mathbf{p}_{e1}=0)e(\mathbf{p}_{e2}=0)$$



Initial state



Final state

Transition amplitude

$$\mathcal{A}_\nu(E, E') = -\langle \Psi_{pp}(E') | V_\nu^{1S_0} | \Psi_{nn}(E) \rangle$$

$$E' = E + 2(m_n - m_p - m_e),$$

$$|\mathbf{p}'| = \sqrt{\mathbf{p}^2 + 2m_N(m_n - m_p - m_e)},$$

- 计算跃迁振幅（微扰展开）：

$$V_{NN}^{^1S_0} = C + V_{\pi}^{^1S_0}(\mathbf{q}),$$

Leading-order (领头阶)

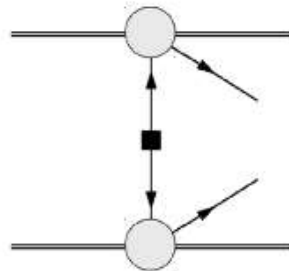
$$V_{\pi}^{^1S_0}(\mathbf{q}) = -\frac{g_A^2}{4F_{\pi}^2} \frac{m_{\pi}^2}{\mathbf{q}^2 + m_{\pi}^2}$$

Nuclear force



$$V_0(\mathbf{q}) = \tilde{C} + V_{\pi}(\mathbf{q}), \quad V_{\pi}(\mathbf{q}) = -\frac{g_A^2}{4F_{\pi}^2} \frac{m_{\pi}^2}{\mathbf{q}^2 + m_{\pi}^2},$$

Neutrino potential



$$V_{\nu,0}(\mathbf{q}) = \tau^{(1)} + \tau^{(2)} + \frac{1}{\mathbf{q}^2} \left(1 - g_A^2 \boldsymbol{\sigma}^{(1)} \cdot \boldsymbol{\sigma}^{(2)} \right. \\ \left. + g_A^2 \boldsymbol{\sigma}^{(1)} \cdot \mathbf{q} \boldsymbol{\sigma}^{(2)} \cdot \mathbf{q} \frac{2m_{\pi}^2 + \mathbf{q}^2}{(\mathbf{q}^2 + m_{\pi}^2)^2} \right),$$

See Chiral effective field theory and nuclear forces
R. Machleidt, D. R. Entem, Phys. Rep. (2011)

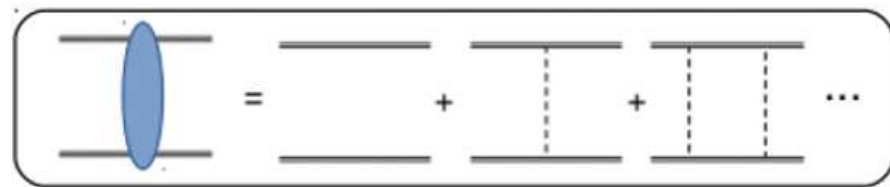
The Lippmann–Schwinger equation for the two-nucleon scattering system

$$\begin{aligned}
 |\psi^{(\pm)}\rangle &= |\phi\rangle + \frac{1}{E - H_0 \pm i\epsilon} V_\pi |\psi^{(\pm)}\rangle \\
 &= |\phi\rangle + \frac{1}{E - H_0 - V_\pi \pm i\epsilon} |\psi^{(\pm)}\rangle \\
 &\equiv |\phi\rangle + G_E |\psi^{(\pm)}\rangle
 \end{aligned}$$

Green function is defined as

$$\begin{aligned}
 \hat{G}_E^\pm &= \frac{1}{E - H_0 - V_\pi \pm i\epsilon}, \\
 G_E^\pm(\mathbf{r}, \mathbf{r}') &= \int \frac{d^3\mathbf{k}}{(2\pi)^3} \int \frac{d^3\mathbf{k}'}{(2\pi)^3} e^{i\mathbf{k}\cdot\mathbf{r}} e^{-i\mathbf{k}'\cdot\mathbf{r}'} \langle \mathbf{k} | \hat{G}_E^\pm | \mathbf{k}' \rangle.
 \end{aligned}$$

“bubble” diagram



$$\begin{aligned}
 |\psi^{(\pm)}\rangle &= |\phi\rangle + \frac{1}{a} b |\psi^{(\pm)}\rangle \\
 &= |\phi\rangle + \frac{1}{a} b \left(|\phi\rangle + \frac{1}{a} b |\psi^{(\pm)}\rangle \right) \\
 &\equiv |\phi\rangle + \frac{1}{a} b |\phi\rangle + \frac{1}{a} b \frac{1}{a} b |\psi^{(\pm)}\rangle \\
 &= |\phi\rangle + \frac{1}{a - b} |\phi\rangle
 \end{aligned}$$

The potential energy V_π describes the interaction between the two colliding systems. The H_0 describes the situation in which the two systems are infinitely far apart and do not interact. Its eigenfunctions $|\phi\rangle$ are and its eigenvalues are the energies E .

- 计算跃迁振幅（微扰展开）：

$$\mathcal{A}_v = - \int d^3\mathbf{r} \psi_{\mathbf{p}'}^-(\mathbf{r})^* V_{vL}^{1S_0}(\mathbf{r}) \psi_{\mathbf{p}}^+(\mathbf{r})$$

in terms of the solutions

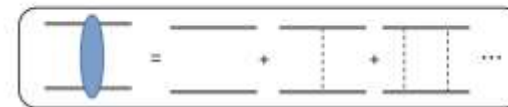
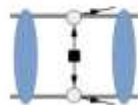
$$\psi_{\mathbf{p}}^{\pm}(\mathbf{r}) = \chi_{\mathbf{p}}^{\pm}(\mathbf{r}) + \chi_{\mathbf{p}}^{\pm}(\mathbf{0}) K_E G_E^{\pm}(\mathbf{r}, 0)$$

w.f. only with bubble

$$\chi_{\mathbf{p}}^{\pm}(\mathbf{r}) = \int \frac{d^3\mathbf{k}}{(2\pi)^3} e^{i\mathbf{k}\cdot\mathbf{r}} \langle \mathbf{k} | (1 + \hat{G}_E^{\pm} V_{\pi}) | \mathbf{p} \rangle.$$

LO

1) Diagram A

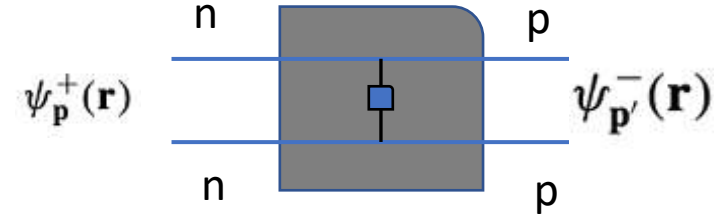


2) Diagram B



$$\mathcal{A}_v^{\text{LO}} = \mathcal{A}_A + \chi_{\mathbf{p}'}^+(\mathbf{0}) K_{E'} \mathcal{A}_B + \bar{\mathcal{A}}_B K_E \chi_{\mathbf{p}}^+(\mathbf{0}) + \chi_{\mathbf{p}'}^+(\mathbf{0}) K_{E'} \mathcal{A}_C K_E \chi_{\mathbf{p}}^+(\mathbf{0}),$$

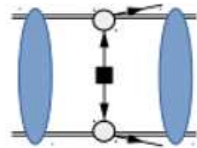
3) Diagram C



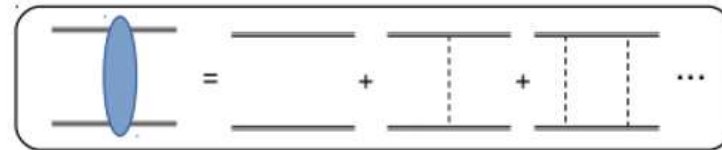
$$K_E = \frac{C}{1 - C G_E^+(\mathbf{0}, \mathbf{0})}.$$

- 计算跃迁振幅（微扰展开）：

1) Diagram A



$$G_E^\pm(\mathbf{r}, \mathbf{r}') = \langle \mathbf{r}' | (E - T - V_\pi \pm i0^+)^{-1} | \mathbf{r} \rangle$$



(i) All diagrams in \mathcal{A}_A are finite. The tree level is finite and each V_π iteration improves the convergence by bringing in a factor of $d^3\mathbf{k}/(\mathbf{k}^2)^2$, where one \mathbf{k}^2 comes from the pion propagator and the other from the two-nucleon propagator.

$$\mathcal{A}_A = - \int d^3\mathbf{r} \chi_{\mathbf{p}'}^-(\mathbf{r})^* V_{\nu L}^{1S_0}(\mathbf{r}) \chi_{\mathbf{p}}^+(\mathbf{r}),$$

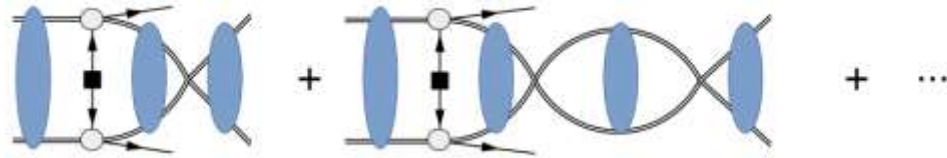
In this coordinate-space picture, the UV convergence or divergence of the amplitudes can be simply recovered from the $r \rightarrow 0$ behavior. For $r \rightarrow 0$, the long-range neutrino potential goes as $1/r$, while the Yukawa wave function $\chi_{\mathbf{p}}^\pm(r)$ tends to a constant. This confirms that \mathcal{A}_A is finite. On the other hand, for the propagator $G_E^\pm(\mathbf{r}, \mathbf{0})$ one has

$$G_E^\pm(\mathbf{r}, \mathbf{0}) \rightarrow \frac{m_N}{4\pi r} + \dots$$

$$\int \frac{1}{r} r^2 dr \quad r \rightarrow 0 \quad \text{UV finite!}$$

- 计算跃迁振幅（微扰展开）：

2) Diagram B



$$\mathcal{A}_B(\mathbf{p}'^2, \mathbf{p}^2) = \bar{\mathcal{A}}_B(\mathbf{p}^2, \mathbf{p}'^2)$$

$$= -m_N \int \frac{d^{d-1}k}{(2\pi)^{d-1}} \frac{1}{\mathbf{p}^2 - \mathbf{k}^2 + i\epsilon} \frac{1 + 3g_A^2}{(\mathbf{k} - \mathbf{p}')^2},$$

(ii) All the diagrams in \mathcal{A}_B and $\bar{\mathcal{A}}_B$ are finite. The first loop goes as $d^3\mathbf{k}/(\mathbf{k}^2)^2$, while V_π insertions further improve the convergence.

坐标表象

$$\mathcal{A}_B + \bar{\mathcal{A}}_B = - \int d^3\mathbf{r} (G_{E'}^-(\mathbf{r}, \mathbf{0})^* V_{\nu L}^{1S_0}(\mathbf{r}) \chi_{\mathbf{p}}^+(\mathbf{r})$$

$$+ \chi_{\mathbf{p}'}^-(\mathbf{r})^* V_{\nu L}^{1S_0}(\mathbf{r}) G_E^+(\mathbf{r}, \mathbf{0})),$$

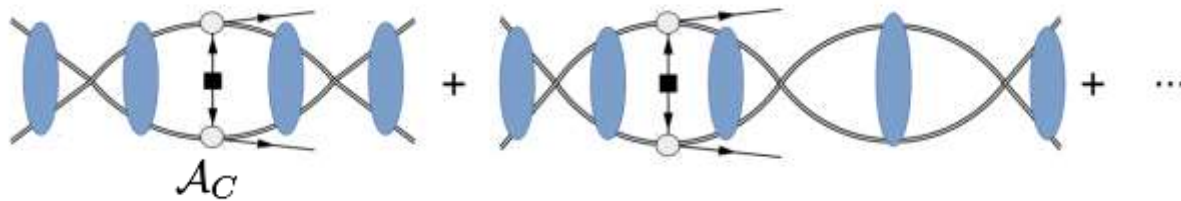
$$G_E^\pm(\mathbf{r}, \mathbf{0}) \rightarrow \frac{m_N}{4\pi r} + \dots$$

$$\int \frac{1}{r^2} r^2 dr \quad r \rightarrow 0$$

UV finite!

- 计算跃迁振幅（微扰展开）：

3) Diagram C (前后都引入短程核力贡献)



$$\mathcal{A}_{\Delta L=2}^{(\nu)} = K_{E'} \mathcal{A}_C K_E \quad K_E = \frac{\chi_{\mathbf{p}}^+(0) \tilde{C}}{1 - \tilde{C} G_E^+(\mathbf{0}, \mathbf{0})}$$

$$= \chi_{\mathbf{p}}^+(0) \tilde{C} + \chi_{\mathbf{p}}^+(0) \tilde{C} \tilde{C} G_E^+(\mathbf{0}, \mathbf{0}) + \dots$$

坐标表象

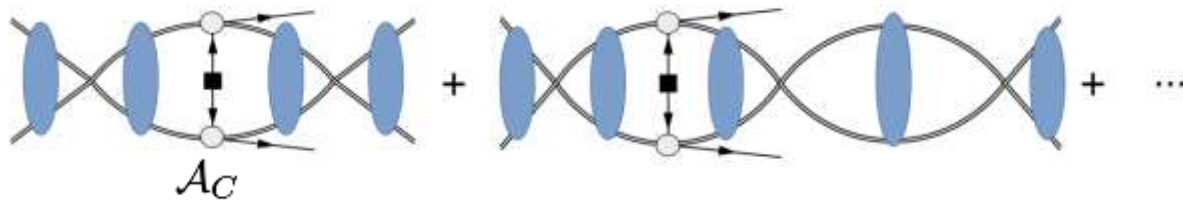
$$\mathcal{A}_C^{\text{sing}} = - \int d^3 \mathbf{r} G_{E'}^{(0)-}(\mathbf{r}, \mathbf{0})^* \tilde{V}_{\nu L}^{1S_0}(\mathbf{r}) G_E^{(0)+}(\mathbf{r}, \mathbf{0}),$$

$$G_E^{(0)\pm}(\mathbf{r}, \mathbf{0}) = -\frac{m_N}{4\pi r} e^{\pm i p r}. \quad (64)$$

$$\int \frac{1}{r^3} r^2 dr \sim \int \frac{1}{r} dr \quad r \rightarrow 0 \quad \text{UV logarithmically divergent}$$

- 计算跃迁振幅（微扰展开）：

3) Diagram C (前后都引入短程核力贡献)

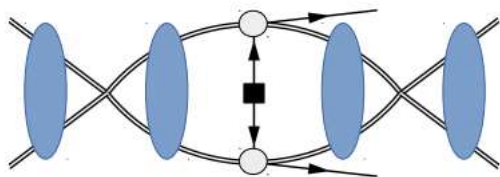


(iii) The first two-loop diagram in \mathcal{A}_C has a logarithmic divergence, which stems from an insertion of the most

$$\mathcal{A}_C(\mathbf{p}^2, \mathbf{p}'^2) = -m_N^2 \int \frac{d^{d-1}k}{(2\pi)^{d-1}} \int \frac{d^{d-1}q}{(2\pi)^{d-1}} \frac{1}{\mathbf{p}^2 - \mathbf{k}^2 + i\epsilon} \\ \times \frac{1 + 3g_A^2}{(\mathbf{k} - \mathbf{q})^2} \frac{1}{\mathbf{p}'^2 - \mathbf{q}^2 + i\epsilon}. \quad (48)$$

$$= -\left(\frac{m_N}{4\pi}\right)^2 \frac{1 + 3g_A^2}{2} \\ \times \left(\frac{1}{4-d} - \gamma + \ln 4\pi + 2L_{\mathbf{p}, \mathbf{p}'}(\mu) \right), \quad L_{\mathbf{p}, \mathbf{p}'}(\mu) = \frac{1}{2} \left[\ln \frac{\mu^2}{-4(|\mathbf{p}| + |\mathbf{p}'|)^2 - i\epsilon} + 1 \right].$$

发散项

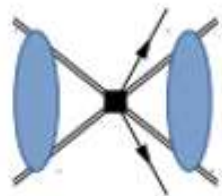
维数正规化方法 $\int d^4 q \rightarrow \int d^d q$

$$\mathcal{A}_C^{(\text{div})} = - \left(\frac{m_N}{4\pi} \right)^2 (1 + 2g_A^2) \left[\Delta + L_{\mathbf{p}, \mathbf{p}'}(\mu) \right],$$

$$L_{\mathbf{p}, \mathbf{p}'}(\mu) = \frac{1}{2} \left(\log \frac{\mu^2}{-(|\mathbf{p}| + |\mathbf{p}'|)^2 + i0^+} + 1 \right),$$

where $\Delta \equiv (1/(4-d) - \gamma + \log 4\pi)/2$. The divergence for $d \rightarrow 4$ can be removed by introducing g_ν^{NN} at LO.

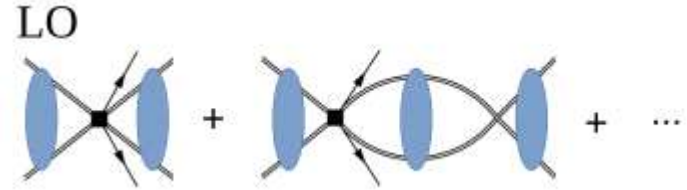
重整化：引入抵消项



$$\mathcal{A}_{\Delta L=2}^{(NN)} = K_{E'} \frac{2g_\nu^{NN}}{\tilde{C}^2} K_E,$$

4) CT(SR) contribution

$$V_{\nu S}(\mathbf{p}, \mathbf{p}') = -2\tau^{(1)+}\tau^{(2)+}\left(g_{\nu}^{NN} + g_{2\nu}^{NN}\frac{\mathbf{p}^2 + \mathbf{p}'^2}{2}\right)$$



跃迁振幅 $\mathcal{A}_C = \mathcal{A}_C^{(\text{div})} + \delta\mathcal{A}_C.$

引入抵消项后 $\mathcal{A}_C \rightarrow \delta\mathcal{A}_C + \left(\frac{m_N}{4\pi}\right)^2 \left[2\tilde{g}_{\nu}^{NN}(\mu) - (1 + 2g_A^2) L_{\mathbf{p},\mathbf{p}'}(\mu)\right]$

$$\tilde{g}_{\nu}^{NN} = \left(\frac{4\pi}{m_N\tilde{C}}\right)^2 g_{\nu}^{NN}$$

代入重整化群方程 (RGE) $\frac{d\mathcal{A}_C}{d\ln\mu} = \mu \frac{d\mathcal{A}_C}{d\mu} = 0$

(散射振幅不依赖能量标度 μ)

得到 $\frac{d}{d\ln\mu}\tilde{g}_{\nu}^{NN} = \frac{1 + 3g_A^2}{2} \equiv \beta.$


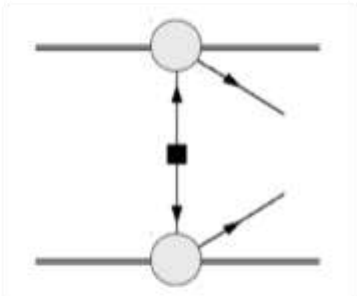
因此, $\tilde{g}_{\nu}^{NN} \sim \mathcal{O}(1)$

The solution is

$$\tilde{g}_{\nu}^{NN}(\mu) = \beta \ln(\mu/\mu_0) + \tilde{g}_{\nu}^{NN}(\mu_0),$$

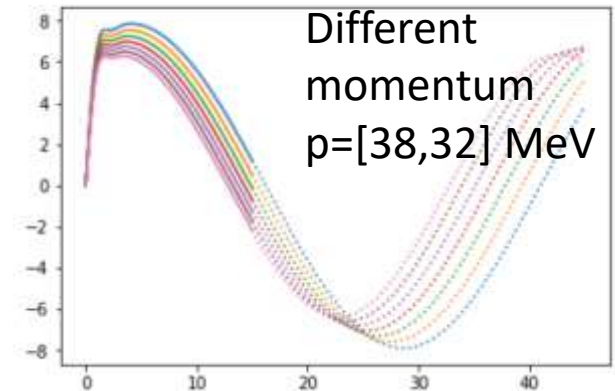
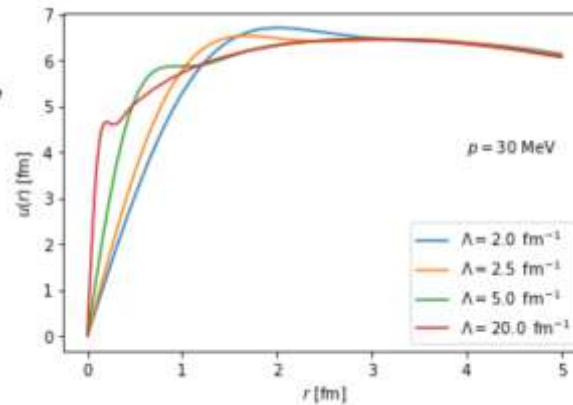
LO contribution

在坐标空间计算跃迁振幅（非微扰方法求解）：

Nuclear force		$V_0(\mathbf{q}) = \tilde{C} + V_\pi(\mathbf{q}), \quad V_\pi(\mathbf{q}) = -\frac{g_A^2}{4F_\pi^2} \frac{m_\pi^2}{\mathbf{q}^2 + m_\pi^2},$
Neutrino potential		$V_{\nu,0}(\mathbf{q}) = \tau^{(1)+}\tau^{(2)+} + \frac{1}{\mathbf{q}^2} \left(1 - g_A^2 \boldsymbol{\sigma}^{(1)} \cdot \boldsymbol{\sigma}^{(2)} + g_A^2 \boldsymbol{\sigma}^{(1)} \cdot \mathbf{q} \boldsymbol{\sigma}^{(2)} \cdot \mathbf{q} \frac{2m_\pi^2 + \mathbf{q}^2}{(\mathbf{q}^2 + m_\pi^2)^2} \right),$
Transition amplitude	$\mathcal{A}_\nu(E, E') = -\langle \Psi_{pp}(E') V_{\nu L}^1 S_0 \Psi_{nn}(E) \rangle$	

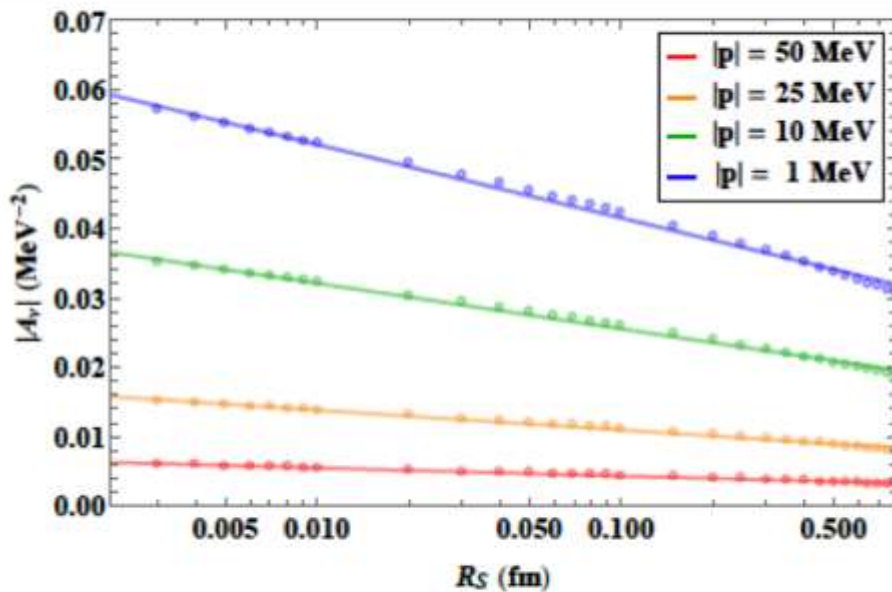
Regulator $\tilde{C} \delta^{(3)}(\mathbf{r}) \rightarrow \frac{\tilde{C}(R_S)}{(\sqrt{\pi} R_S)^3} \exp\left(-\frac{r^2}{R_S^2}\right) \equiv \tilde{C}(R_S) \delta_{R_S}^{(3)}(\mathbf{r})$

$$u_p(r) = rR(r) \rightarrow \frac{1}{p} \sin[pr + \delta(p)],$$



Transition amplitude

$$\mathcal{A}_\nu(E, E') = -\langle \Psi_{pp}(E') | V_\nu^{1S_0} | \Psi_{nn}(E) \rangle$$



- The transition amplitude is regulator dependent!
- Needs a counter term (contact operator) at LO in order to ensure renormalizability.

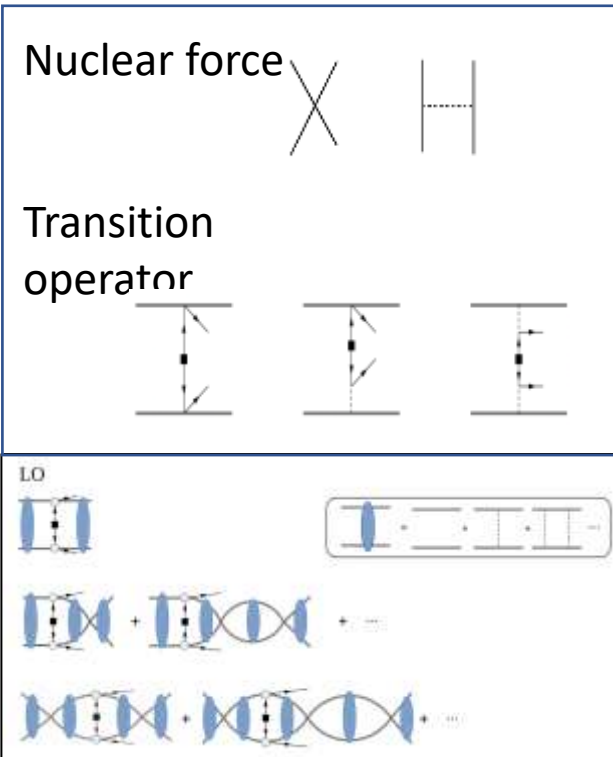
Lines fitted to $\mathcal{A}_\nu = a + b \ln R_S$
 logarithmic dependence on R_S

New Leading Contribution to Neutrinoless Double- β Decay

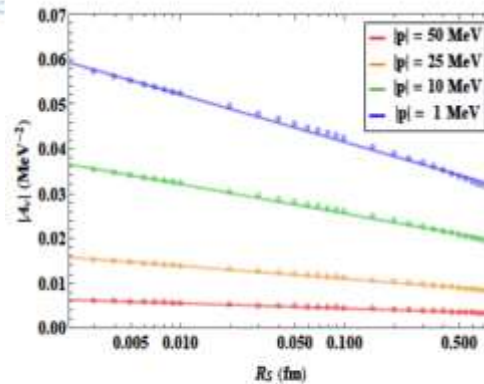
Vincenzo Cirigliano, Wouter Dekens, Jordy de Vries, Michael L. Graesser, Emanuele Mereghetti, Saori Pastore, and Ubirajara van Kolck

Phys. Rev. Lett. **120**, 202001 – Published 16 May 2018

Physics See Synopsis: [A Missing Piece in the Neutrinoless Beta-Dec](#)



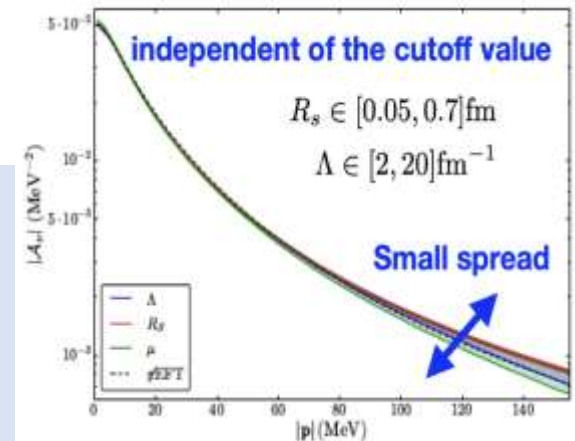
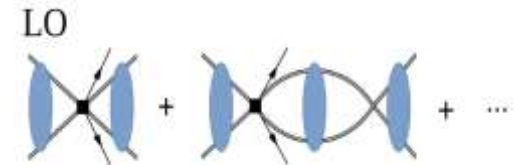
UV divergent

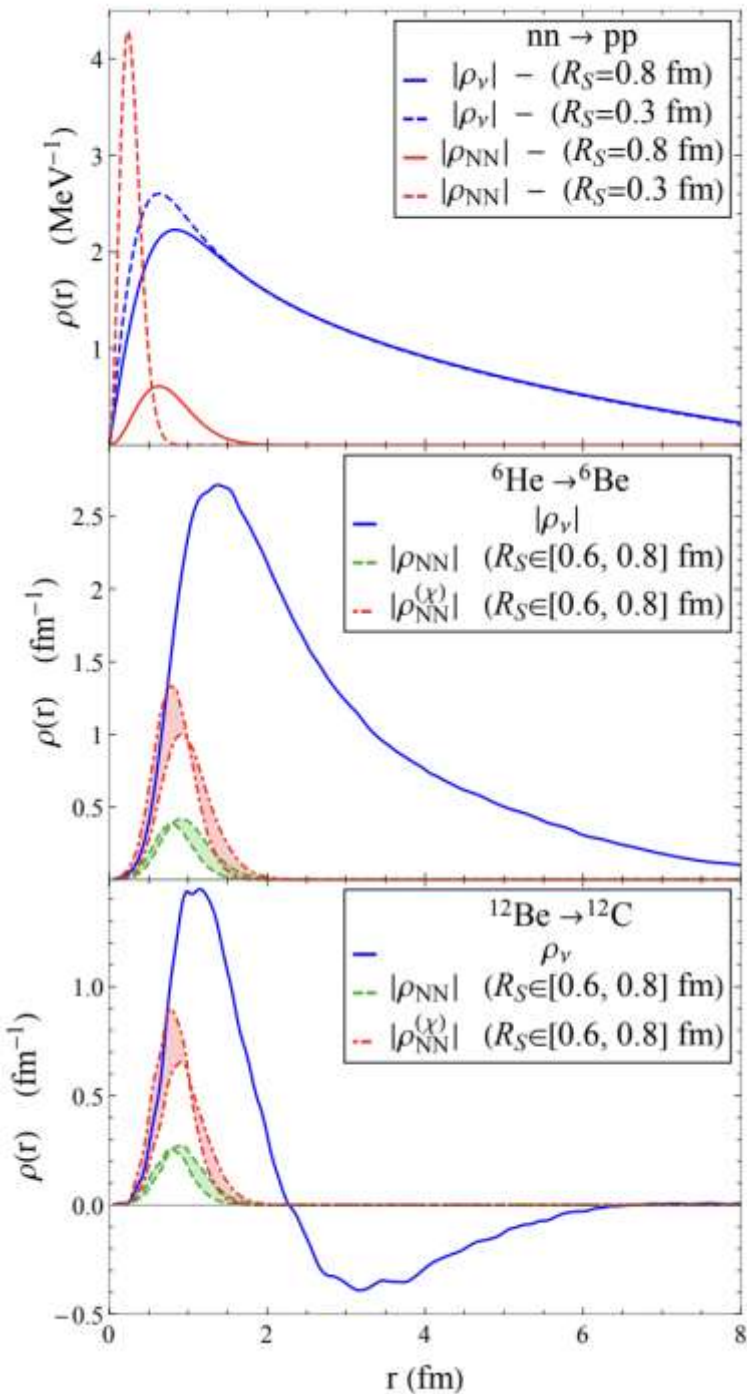


- The transition amplitude is regulator-dependent!
- Needs a counter term at LO in order to ensure renormalizability.

Introducing a contact transition operator

$$V_{\nu,S} = -2g_{\nu}^{NN} \tau^{(1)+} \tau^{(2)+}$$





For $\Delta I = 0$ transitions such as the ${}^6\text{He} \rightarrow {}^6\text{Be}$ shown in Fig. 3 (middle panel), we find $\mathcal{A}_{\Delta L=2}^{(NN)}/\mathcal{A}_{\Delta L=2}^{(\nu)} \sim 10\%$, similarly to the $nn \rightarrow ppee$ case. In realistic $0\nu\beta\beta$ transitions, however, the total nuclear isospin changes by two units, $\Delta I = 2$. This implies the presence of a node in $\rho_\nu(r)$ due to the orthogonality of the initial and final spatial wavefunctions. The resulting partial cancellation between the regions with $r \lesssim 2$ fm and $r \gtrsim 2$ fm [51] leads to a relative enhancement of the short-range contribution, as illustrated in Fig. 3 (bottom panel) for ${}^{12}\text{Be} \rightarrow {}^{12}\text{C}$. Numerically we find $\mathcal{A}_{\Delta L=2}^{(NN)}/\mathcal{A}_{\Delta L=2}^{(\nu)} \sim 25\%$ (our fit),

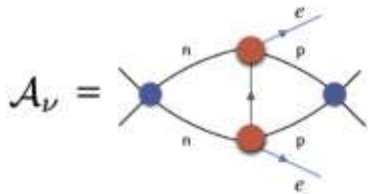
Toward Complete Leading-Order Predictions for Neutrinoless Double β Decay

Vincenzo Cirigliano, Wouter Dekens, Jordy de Vries, Martin Hoferichter, and Emar Mereghetti

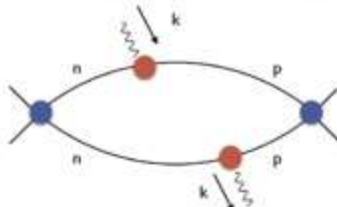
Phys. Rev. Lett. **126**, 172002 (2021) – Published 30 April 2021

- **Cottingham formula** W.N. Cottingham, Ann. Phys. 25, 424 (1963)

$$\mathcal{A}_\nu \propto \int \frac{d^4 k}{(2\pi)^4} \frac{g_{\mu\nu}}{k^2 + i\epsilon} \int d^4 x e^{ik \cdot x} \langle pp | T \{ j_w^\mu(x) j_w^\nu(0) \} | nn \rangle$$



$$\propto \int \frac{d^4 k}{(2\pi)^4} \frac{1}{k^2 + i\epsilon}$$



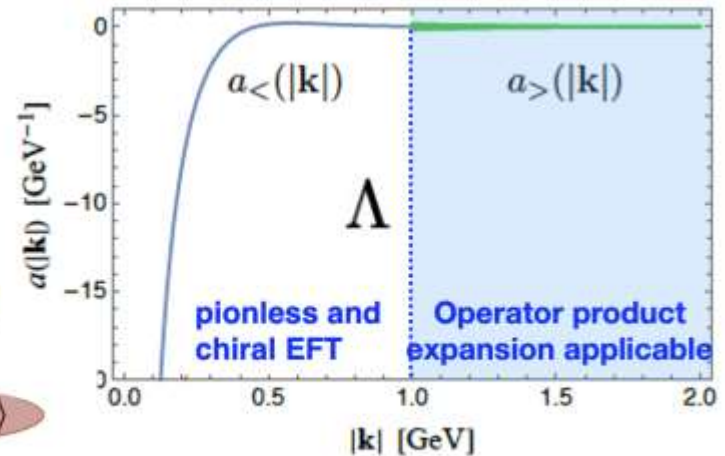
forward Compton amplitude

- **Synthetic datum**

$$\mathcal{A}_\nu(|\mathbf{p}|, |\mathbf{p}'|) \times e^{-i(\delta_{1S_0}(|\mathbf{p}|) + \delta_{1S_0}(|\mathbf{p}'|))} = - \left(2.271 - 0.075 \tilde{c}_1(4 M_\pi) \right) \times 10^{-2} \text{ MeV}^{-2}$$

$$|\mathbf{p}| = 25 \text{ MeV} \quad (|\mathbf{p}'| = 30 \text{ MeV}) \quad = -1.95(5) \tilde{c}_1 \times 10^{-2} \text{ MeV}^{-2},$$

Uncertainty from the estimate of the **inelastic** contributions



$$\mathcal{A}_\nu^{\text{full}} = \int_0^\infty d|k| a^{\text{full}}(|k|) = \mathcal{A}^< + \mathcal{A}^>, \quad \Lambda$$

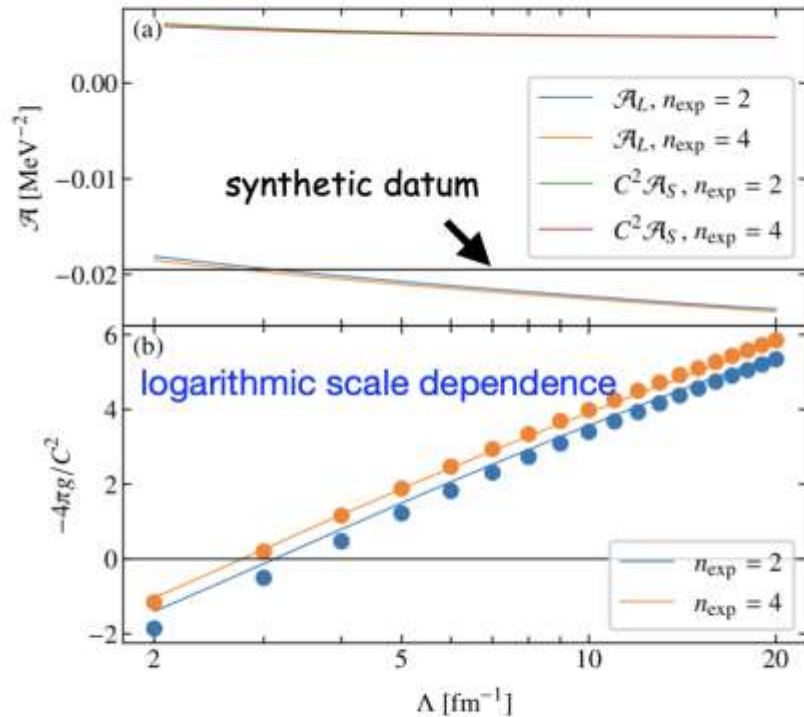
$$\mathcal{A}^< = \int_0^\Lambda d|k| a_<(|k|),$$

$$\mathcal{A}^> = \int_\Lambda^\infty d|k| a_>(|k|),$$

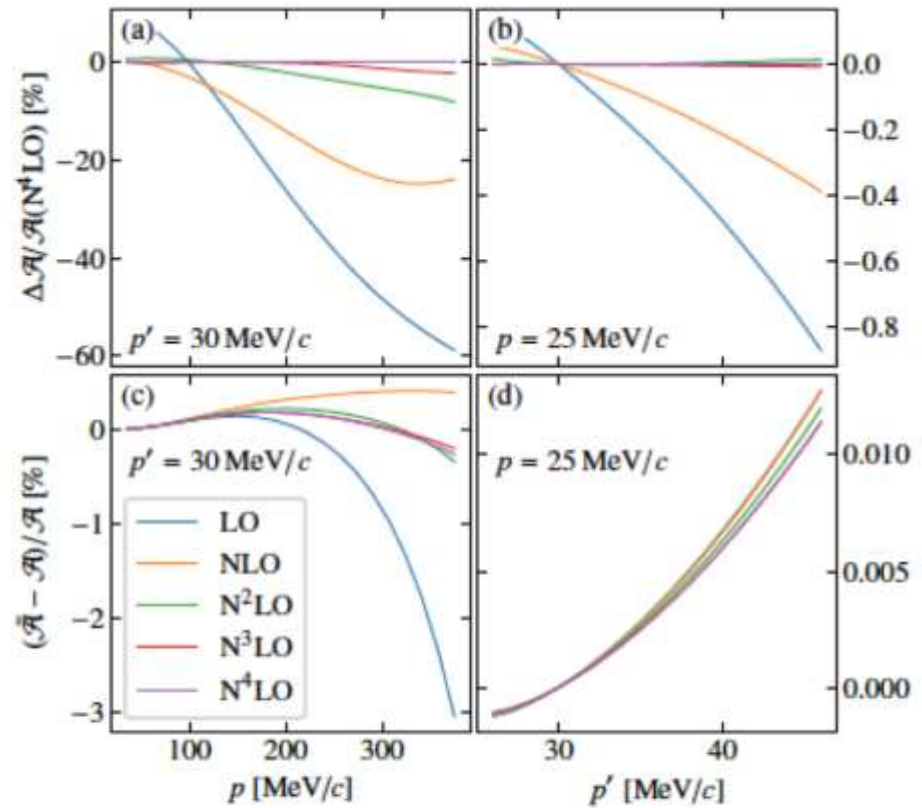
The transition amplitude is observable and thus scheme independent.

$$\mathcal{A}(p, p') = 4\pi \left\langle {}^1S_0(p') \left| V_{v,L}^1 S_0 + V_{v,S}^1 S_0 \right| {}^1S_0(p) \right\rangle$$

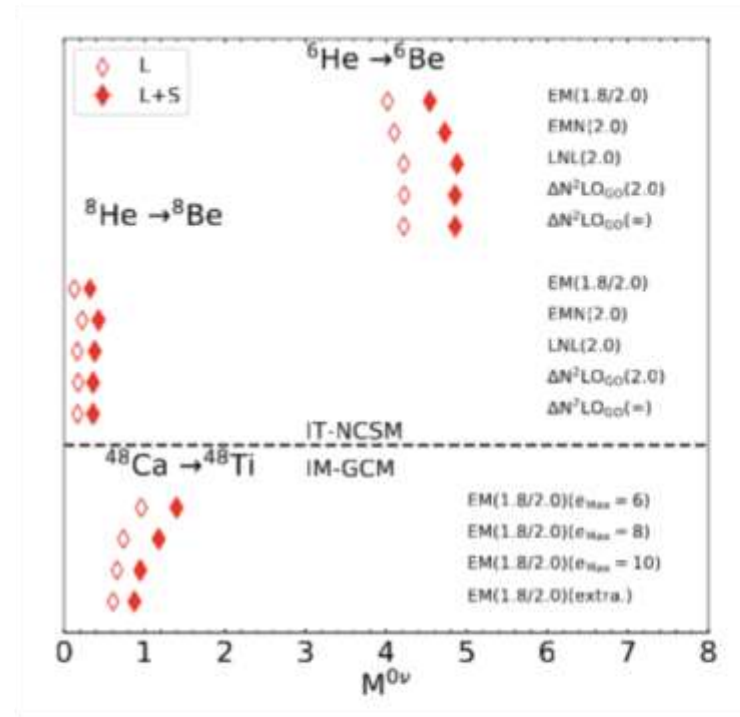
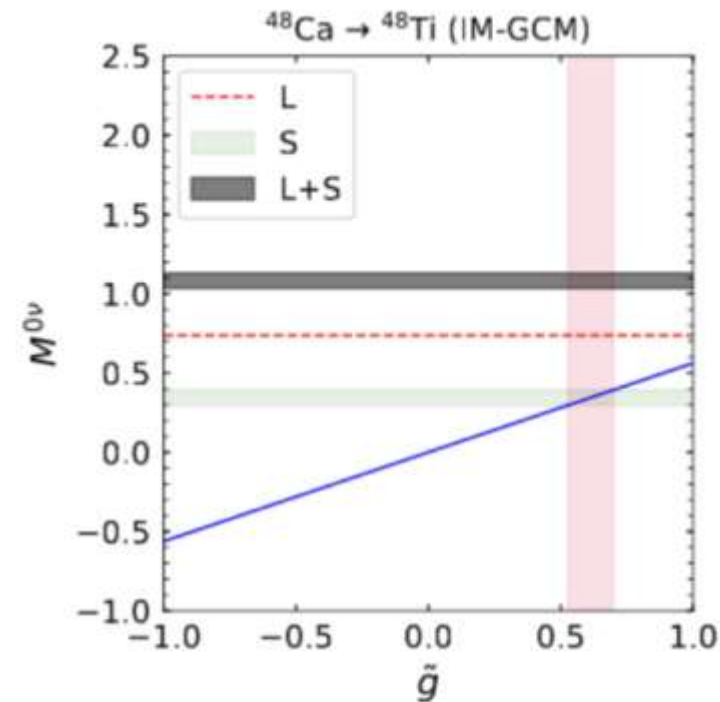
$$\mathcal{A}(p, p') = \mathcal{A}_L(p, p') - 2g\mathcal{A}_S(p, p').$$



The dimensionless LEC C is adjusted to reproduce the neutron-proton scattering length $a_{np} = -23.74$ fm.



- expansion order of the chiral nuclear force (not transition operator)
- LO and N²LO (partial) neutrino potential



- ▶ The contact term **enhances the NME for ^{48}Ca by 43(7)%**, the uncertainty is propagated only from the synthetic datum.
- ▶ An important positive message for planning and interpreting future experiments.

现在回到这篇论文的内容。

Relativistic framework.—We start from a manifestly Lorentz-invariant effective Lagrangian relevant at the leading order of chiral EFT [19],

$$\mathcal{L}_{\Delta L=0} = \frac{f_\pi^2}{4} \text{tr}[u_\mu u^\mu + m_\pi^2(uu + u^\dagger u^\dagger)] \\ + \bar{\Psi}(i\gamma^\mu D_\mu - M + \frac{g_A}{2}\gamma^\mu \gamma_5 u_\mu)\Psi - \sum_\alpha \frac{C_\alpha}{2}(\bar{\Psi}\Gamma_\alpha\Psi)^2,$$

通过SU(2)群表示引入pion 场

$$u = \exp[i\vec{\tau} \cdot \vec{\pi}/(2f_\pi)]$$

与轻子流耦合: axial vector $u_\mu = iu^\dagger(\partial_\mu - il_\mu)u - iu\partial_\mu u^\dagger$

协变微商: $D_\mu = \partial_\mu + \frac{1}{2}[u^\dagger(\partial_\mu - il_\mu)u + u\partial_\mu u^\dagger].$

$$l_\mu = -2\sqrt{2}G_F V_{ud}\tau^+ \bar{e}_L \gamma_\mu \nu_{eL}$$

[19] Chiral effective field theory and nuclear forces

R. Machleidt, D. R. Entem, Phys. Rep. (2011)

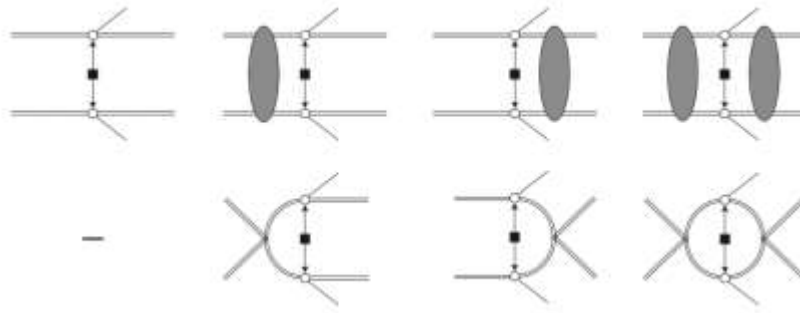


FIG. 1. Leading-order contributions to the amplitude of $nn \rightarrow ppe^-e^-$ (first row) and the corresponding ultraviolet divergence structures (second row). The double and plain lines denote nucleon and lepton fields, respectively. The squares denote an insertion of neutrino potential V_ν . The circles denote the nucleon axial and vector currents coupled to V_ν . The gray ellipses represent the T matrix generated by iteration of the strong potential V_s .

Contrary to the previous studies based on the heavy baryon approach [27, 28], which relies on a nonrelativistic expansion of the Lagrangian, here we apply the manifestly Lorentz-invariant Lagrangian to the problem of $0\nu\beta\beta$ decay. The LO contribution to the scattering amplitude can be obtained by solving the relativistic scattering equation

$$T(\mathbf{p}', \mathbf{p}) = V(\mathbf{p}', \mathbf{p}) + \int \frac{d^3k}{(2\pi)^3} \frac{M^2}{\mathbf{k}^2 + M^2} \frac{V(\mathbf{p}', \mathbf{k})T(\mathbf{k}, \mathbf{p})}{E - 2\sqrt{\mathbf{k}^2 + M^2} + i0^+}, \quad (3)$$

where E is the total energy, and \mathbf{p}' and \mathbf{p} are the nucleon outgoing and incoming momenta in the center of mass frame, respectively.

As a result, the LO strong and neutrino potentials take the form as those in the Weinberg's approach,

$$V_s(\mathbf{p}', \mathbf{p}) = -\frac{g_A^2}{4f_\pi^2} \vec{\tau}_1 \cdot \vec{\tau}_2 \frac{\boldsymbol{\sigma}_1 \cdot \mathbf{q} \boldsymbol{\sigma}_2 \cdot \mathbf{q}}{q^2 + m_\pi^2} + C_1 + C_2 \boldsymbol{\sigma}_1 \cdot \boldsymbol{\sigma}_2, \quad (4)$$

$$V_\nu(\mathbf{p}', \mathbf{p}) = \frac{\tau_1^+ \tau_2^+}{q^2} \left[1 - g_A^2 \boldsymbol{\sigma}_1 \cdot \boldsymbol{\sigma}_2 + g_A^2 \boldsymbol{\sigma}_1 \cdot \mathbf{q} \boldsymbol{\sigma}_2 \cdot \mathbf{q} \frac{2m_\pi^2 + q^2}{(q^2 + m_\pi^2)^2} \right], \quad (5)$$

where $\mathbf{q} = \mathbf{p}' - \mathbf{p}$, and $C_1 = C_S + C_V$ and $C_2 = -C_{AV} + 2C_T$ are two independent LECs.

$$T(\mathbf{p}', \mathbf{p}) = V(\mathbf{p}', \mathbf{p}) + \int \frac{d^3k}{(2\pi)^3} \frac{M^2}{\mathbf{k}^2 + M^2} \frac{V(\mathbf{p}', \mathbf{k})T(\mathbf{k}, \mathbf{p})}{E - 2\sqrt{\mathbf{k}^2 + M^2} + i0^+}, \quad (3)$$

Note that the present derivation is similar to the so-called modified Weinberg approach [54], which was applied to nucleon-nucleon scattering problem. It has proven to be useful to improve the renormalizability of nucleon-nucleon scattering [54] and few-body systems [55, 56]. In the heavy baryon approach, the non-relativistic expansion of the Lagrangian leads, instead of Eq. (3), to the Lippmann-Schwinger equation, which contains a nonrelativistic limit ($1/M \rightarrow 0$) of the two-nucleon propagator

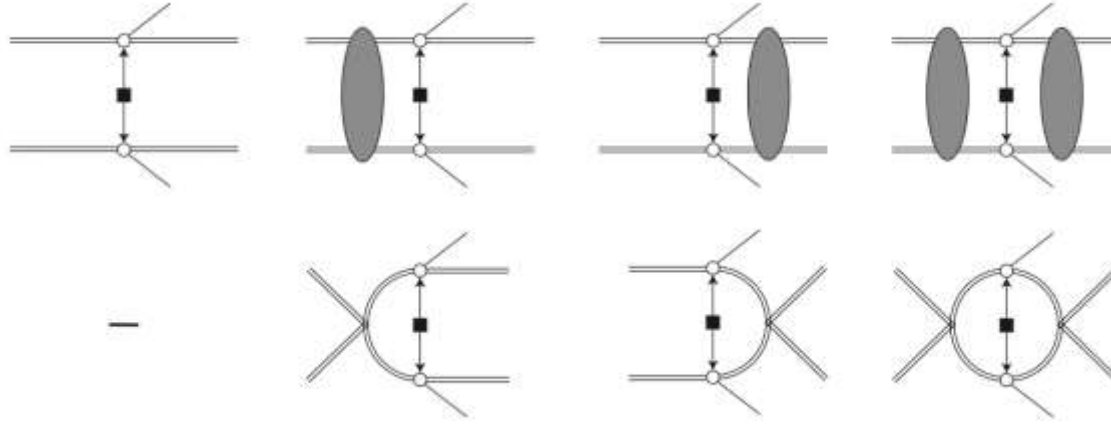
$$\frac{M^2}{\mathbf{k}^2 + M^2} \xrightarrow{=1} \frac{1}{E - 2\sqrt{\mathbf{k}^2 + M^2} + i0^+} \rightarrow \frac{1}{E_{\text{kin}} - \mathbf{k}^2/M + i0^+}. \quad (6)$$

Obviously, the relativistic propagator scales as $\mathcal{O}(\Lambda^{-3})$ at the ultraviolet (UV) region $|\mathbf{k}| \sim \Lambda$, while the nonrelativistic one scales as $\mathcal{O}(\Lambda^{-2})$. As a result of this milder UV behavior, we will show that the $0\nu\beta\beta$ amplitude can be renormalized without promoting a contact term to the LO neutrino potential.

Note: E is the energy of two nucleons !

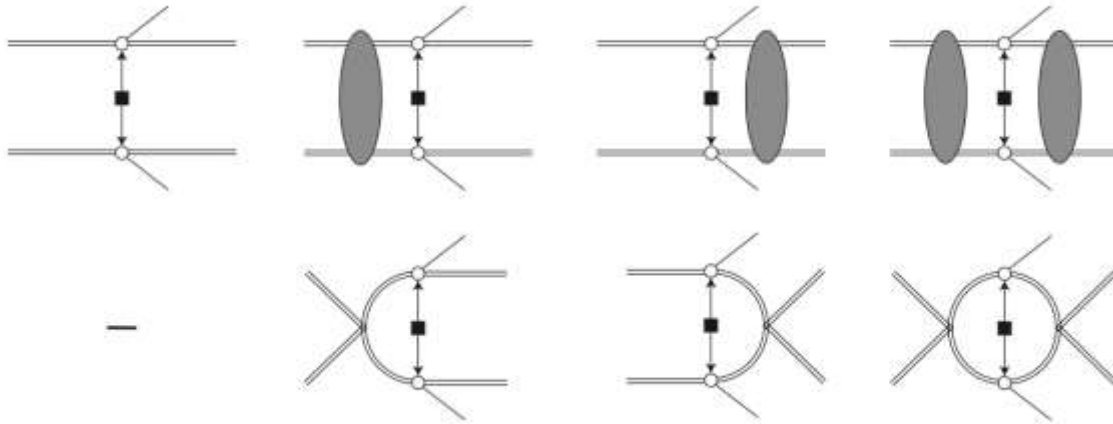
$$\begin{aligned} E - 2(k^2 + M^2)^{1/2} &= E - 2M(1 + k^2/M^2)^{1/2} \\ &= E - 2M(1 + \frac{k^2}{2M^2} + \dots) \\ &\simeq E_k - \frac{k^2}{M} \end{aligned}$$

Note: E_k is the kinetic energy of two nucleons !



$$\mathcal{A}_\nu^{\text{LO}} = -\rho_{fi}(V_\nu + V_\nu G_0 T_s + T_s G_0 V_\nu + T_s G_0 V_\nu G_0 T_s), \quad (7)$$

where $\rho_{fi} = M^2 / \sqrt{(\mathbf{p}_f^2 + M^2)(\mathbf{p}_i^2 + M^2)}$ is a phase space factor [57], G_0 the two-nucleon free propagator, and T_s the T -matrix resumming the strong potential V_s . The four terms in Eq. (7) correspond to the four diagrams depicted in the first row of Fig. 1, and here we denote them as \mathcal{A}_A , \mathcal{A}_B , $\bar{\mathcal{A}}_B$, and \mathcal{A}_C from left to right.



the diagrams $\mathcal{A} \sim \mathcal{O}(\Lambda^D)$ ($\log \Lambda$ for $D = 0$). The \mathcal{A}_A tree diagram has no divergence. For \mathcal{A}_B , $\bar{\mathcal{A}}_B$, and \mathcal{A}_C , it was shown that the degree of divergence is dominated by the loop integrals involving the insertion of neutrino potential, once T_s is made finite [27]. The divergence structures are shown in the second row of Fig. 1. Counting the powers of loop momenta, one finds the degree of divergence

$$D = L(3 + g) - 2 \quad (8)$$

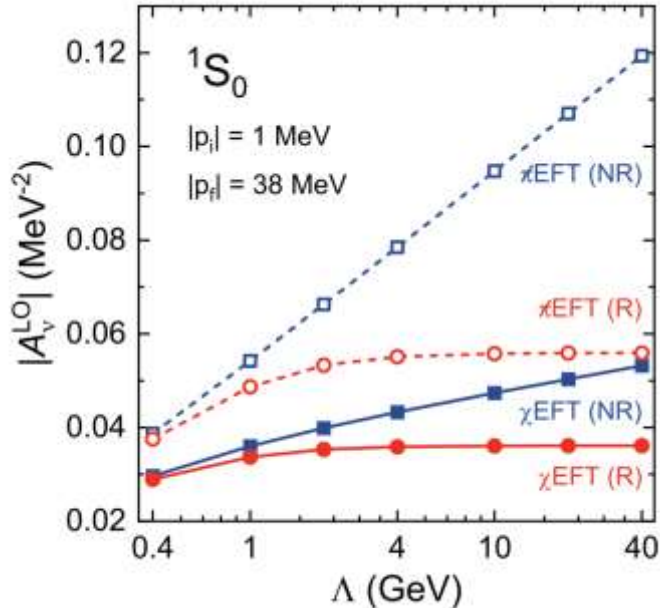
with L being the number of loops and g the UV scaling of the two-nucleon propagator, and -2 comes from the $|\mathbf{q}|^{-2}$ dependence of V_ν .

From Eq. (6), we know the nonrelativistic propagator has $g = -2$ and the relativistic one has $g = -3$. Therefore, in the nonrelativistic framework, \mathcal{A}_B and $\bar{\mathcal{A}}_B$ are convergent as $\mathcal{O}(\Lambda^{-1})$, but \mathcal{A}_C is logarithmic divergent. In the present relativistic framework, however, \mathcal{A}_B , $\bar{\mathcal{A}}_B$, and \mathcal{A}_C are all convergent as $\mathcal{O}(\Lambda^{-2})$, so the corresponding LO amplitude is renormalizable. Such analysis should

The renormalizability of the LO amplitude $\mathcal{A}_\nu^{\text{LO}}$ can be demonstrated explicitly in any specific regularization scheme. Here, we regulate the strong potential with a separable gaussian function,

$$V_s(\mathbf{p}', \mathbf{p}) \rightarrow e^{-|\mathbf{p}'|^4/\Lambda^4} V_s(\mathbf{p}', \mathbf{p}) e^{-|\mathbf{p}|^4/\Lambda^4}. \quad (9)$$

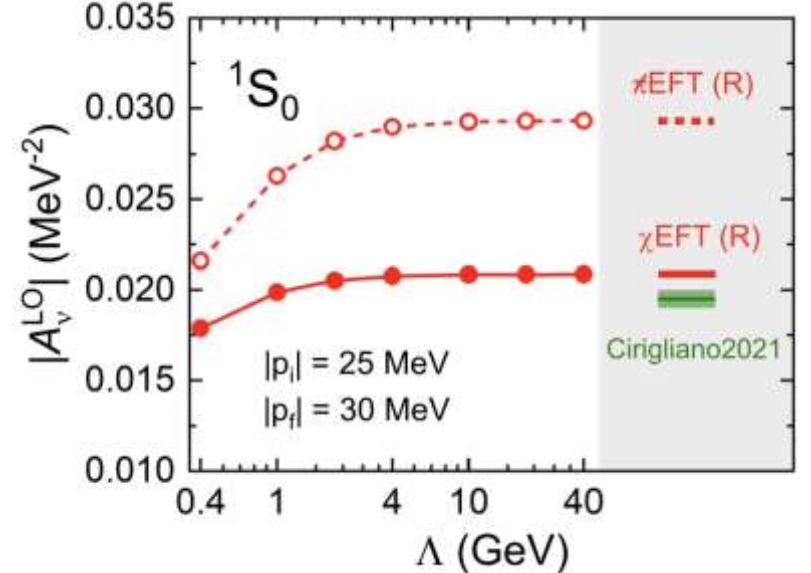
After projecting to the 1S_0 channel, the LEC in its short-range part $C^{^1S_0} = C_1 - 3C_2$ is determined by reproducing the scattering length $a_{np} = -23.74$ fm. We have checked that the 1S_0 phase shifts are indeed cutoff independent as $\Lambda \rightarrow \infty$. Then, the amplitude is evaluated with Eq. (7) in the momentum space.

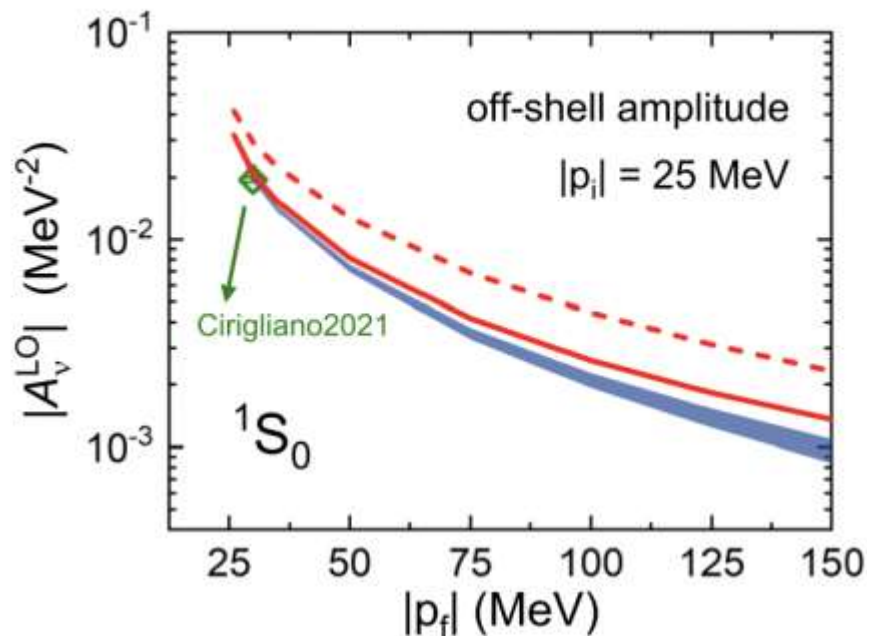


in the previous estimation [29, 30], one has to renormalize the amplitude by introducing an unknown contact term, whose size was constrained by additional model-dependent inputs within a certain range.

It is remarkable that the renormalized amplitude obtained with the relativistic chiral EFT is quite consistent with the previous estimation [29, 30], and their difference is only about 10%. This demonstrates the validity of both approaches for $0\nu\beta\beta$ transitions, but the present relativistic framework avoids the uncertainties introduced by the model-dependent inputs.

Compared to the relativistic chiral EFT, its pion-





With the fitted contact term, the nonrelativistic amplitudes at other kinematic points can also be renormalized. The uncertainty of the synthetic datum reflects its systematic error from the model dependence, which is in turn propagated to the amplitudes given by the nonrelativistic chiral EFT. In contrast, the present relativistic framework provides a model-free prediction of the amplitudes, and they are generally consistent with the nonrelativistic estimations. The relativistic results are slightly larger than the nonrelativistic ones by about 10%-20% for the on-shell amplitude, while for the off-shell amplitude, the enhancement becomes more sizable especially at high final momentum, e.g., about 40% at $|\mathbf{p}_f| = 150$ MeV. This should be understandable because the contact term in the nonrelativistic framework is determined at extremely low-energy kinematics.

FIG. 4. (Color online). The renormalized on-shell (upper) and off-shell (lower) amplitudes $\mathcal{A}_\nu^{\text{LO}}$ at various kinematic points. The blue band represents the nonrelativistic results, in which the contact term is fitted to the synthetic datum (shown as diamond) for the amplitude at kinematics $|\mathbf{p}_i| = 25$ MeV and $|\mathbf{p}_f| = 30$ MeV, i.e., $\mathcal{A}_\nu^{\text{LO}} = -0.0195(5)$ MeV $^{-2}$ [29]. The width of the band reflects the uncertainty propagated from the synthetic datum.

Summary and Outlooks.—We present a model-free prediction of the $nn \rightarrow ppe^-e^-$ amplitude by developing a relativistic framework based on chiral EFT. Contrary to the nonrelativistic case, we show that the amplitude can be renormalized at LO without any uncertain contact operators. The calculated amplitude is slightly larger than the previous model-dependent estimation at the kinematics $|\mathbf{p}_i| = 25$ MeV and $|\mathbf{p}_f| = 30$ MeV [29, 30] by about 10%, providing a highly nontrivial validation for the previous result. The enhancement of the amplitude could be more sizable for either off-shell amplitude or high-momentum kinematics. Therefore, the present am-

Important points:

- 1) When k (q) is sufficiently large, the relativistic framework provides a better description of the dispersion relation.
- 2) In the full relativistic frameworks, no need to introduce the CT term.

Question: How to understand many-body problems in relativistic frameworks (not mean-field approximation)?

→ Test of this conclusion in light nuclei? refit the LEC of CT term.

Thanks for your attention.

$$\begin{cases} q_L \mapsto q'_L = Lq_L = \exp\left(-i\boldsymbol{\theta}_L \cdot \frac{\boldsymbol{\tau}}{2}\right)q_L \\ q_R \mapsto q'_R = Rq_R = \exp\left(-i\boldsymbol{\theta}_R \cdot \frac{\boldsymbol{\tau}}{2}\right)q_R \end{cases}$$

To construct a [non-linear realization](#) of $SO(4)$, the representation describing four-dimensional rotations of a vector

$$\begin{pmatrix} \boldsymbol{\pi} \\ \sigma \end{pmatrix} \equiv \begin{pmatrix} \pi_1 \\ \pi_2 \\ \pi_3 \\ \sigma \end{pmatrix},$$

for an infinitesimal rotation parametrized by six angles

$$\{\theta_i^{V,A}\}, \quad i = 1, 2, 3,$$

is given by

$$\begin{pmatrix} \boldsymbol{\pi} \\ \sigma \end{pmatrix} \xrightarrow{SO(4)} \begin{pmatrix} \boldsymbol{\pi}' \\ \sigma' \end{pmatrix} = \left[\mathbf{1}_4 + \sum_{i=1}^3 \theta_i^V V_i + \sum_{i=1}^3 \theta_i^A A_i \right] \begin{pmatrix} \boldsymbol{\pi} \\ \sigma \end{pmatrix}$$

where

$$\sum_{i=1}^3 \theta_i^V V_i = \begin{pmatrix} 0 & -\theta_3^V & \theta_2^V & 0 \\ \theta_3^V & 0 & -\theta_1^V & 0 \\ -\theta_2^V & \theta_1^V & 0 & 0 \\ 0 & 0 & 0 & 0 \end{pmatrix} \quad \sum_{i=1}^3 \theta_i^A A_i = \begin{pmatrix} 0 & 0 & 0 & \theta_1^A \\ 0 & 0 & 0 & \theta_2^A \\ 0 & 0 & 0 & \theta_3^A \\ -\theta_1^A & -\theta_2^A & -\theta_3^A & 0 \end{pmatrix}.$$

To switch from the above linear realization of $SO(4)$ to the nonlinear one, we observe that, in fact, only three of the four components of $(\boldsymbol{\pi}, \sigma)$ are independent with respect to four-dimensional rotations. These three independent components correspond to coordinates on a hypersphere S^3 , where $\boldsymbol{\pi}$ and σ are subjected to the constraint

$$\boldsymbol{\pi}^2 + \sigma^2 = F^2,$$

with F a ([pion decay](#)) constant of dimension mass.

Utilizing this to eliminate σ yields the following transformation properties of $\boldsymbol{\pi}$ under $SO(4)$,

$$\begin{cases} \theta^V : \boldsymbol{\pi} \mapsto \boldsymbol{\pi}' = \boldsymbol{\pi} + \boldsymbol{\theta}^V \times \boldsymbol{\pi} \\ \theta^A : \boldsymbol{\pi} \mapsto \boldsymbol{\pi}' = \boldsymbol{\pi} + \boldsymbol{\theta}^A \sqrt{F^2 - \boldsymbol{\pi}^2} \end{cases} \quad \boldsymbol{\theta}^{V,A} \equiv \left\{ \theta_i^{V,A} \right\}, \quad i = 1, 2, 3.$$

The nonlinear terms (shifting $\boldsymbol{\pi}$) on the right-hand side of the second equation underlie the nonlinear realization of $SO(4)$. The chiral group $SU(2)_L \times SU(2)_R \simeq SO(4)$ is realized nonlinearly on the triplet of pions— which, however, still transform linearly under isospin $SU(2)_V \simeq SO(3)$ rotations parametrized through the angles $\{\boldsymbol{\theta}_V\}$. By contrast, the $\{\boldsymbol{\theta}_A\}$ represent the nonlinear "shifts" (spontaneous breaking).

Through the [spinor map](#), these four-dimensional rotations of $(\boldsymbol{\pi}, \sigma)$ can also be conveniently written using 2x2 matrix notation by introducing the unitary matrix

$$U = \frac{1}{F} (\sigma \mathbf{1}_2 + i \boldsymbol{\pi} \cdot \boldsymbol{\tau}),$$

and requiring the transformation properties of U under chiral rotations to be

$$U \longrightarrow U' = L U R^\dagger,$$

where $\theta_L = \theta_V - \theta_A, \theta_R = \theta_V + \theta_A$.

The transition to the nonlinear realization follows,

$$U = \frac{1}{F} \left(\sqrt{F^2 - \boldsymbol{\pi}^2} \mathbf{1}_2 + i \boldsymbol{\pi} \cdot \boldsymbol{\tau} \right), \quad \mathcal{L}_\pi^{(2)} = \frac{F^2}{4} \langle \partial_\mu U \partial^\mu U^\dagger \rangle,$$

where $\langle \dots \rangle$ denotes the [trace](#) in the flavor space. This is a [non-linear sigma model](#).

Terms involving $\partial_\mu \partial^\mu U$ or $\partial_\mu \partial^\mu U^\dagger$ are not independent and can be brought to this form through partial integration. The constant $F^2/4$ is chosen in such a way that the Lagrangian matches the usual free term for massless scalar fields when written in terms of the pions,

$$\mathcal{L}_\pi^{(2)} = \frac{1}{2} \partial_\mu \boldsymbol{\pi} \cdot \partial^\mu \boldsymbol{\pi} + \frac{1}{2F^2} (\partial_\mu \boldsymbol{\pi} \cdot \boldsymbol{\pi})^2 + \mathcal{O}(\pi^6).$$

It is now a simple exercise to construct the most general chiral-invariant Lagrangian for pions in terms of the matrix U . The building blocks are given by U , U^\dagger and derivatives of these quantities. Notice that since I consider here only global chiral rotations, i.e. L and R do not depend on space-time, the quantities like e.g. $\partial_\mu \partial_\nu U$ transform in the same way as U itself, i.e. according to Eq. (3.27). Chiral invariant terms in the effective Lagrangian terms can be constructed by taking a trace over products of U , U^\dagger and their derivatives. Lorentz invariance implies that the number of derivatives must be even, so that the effective Lagrangian can be written as

$$\mathcal{L}_\pi = \mathcal{L}_\pi^{(2)} + \mathcal{L}_\pi^{(4)} + \dots \quad (3.29)$$

Notice that $\mathcal{L}_\pi^{(0)}$ is simply a constant since $UU^\dagger = \mathbf{1}_{2 \times 2}$. The lowest-order Lagrangian involves just a single term

$$\mathcal{L}_\pi^{(2)} = \frac{F^2}{4} \langle \partial_\mu U \partial^\mu U^\dagger \rangle, \quad (3.30)$$

- Pions build an isospin triplet and thus transform linearly under $SU(2)_V \subset SU(2)_L \times SU(2)_R$ according to the corresponding irreducible representation;
- The chiral group must be realized *nonlinearly*. This follows immediately from the geometrical argument based on the fact that the Lie algebra of $SU(2)_L \times SU(2)_R$ in Eq. (3.20) is isomorphic to that of $SO(4)$. We know that one needs three coordinates in order to construct the smallest non-trivial representation, the so-called fundamental representation, of the three-dimensional rotation group. Similarly, the smallest nontrivial representation of the four-dimensional rotation group $SO(4)$ is four-dimensional. We have, however, only three “coordinates” at our disposal (the triplet of the pion fields)!

To construct a non-linear realization of $SO(4)$ we begin with the usual representation describing four-dimensional rotations of a vector $(\boldsymbol{\pi}, \sigma) \equiv (\pi_1, \pi_2, \pi_3, \sigma)$. For an infinitesimal rotation parametrized by six angles $\{\theta_i^{V,A}\}$, with $i = 1, 2, 3$, we have:

$$\begin{pmatrix} \boldsymbol{\pi} \\ \sigma \end{pmatrix} \xrightarrow{SO(4)} \begin{pmatrix} \boldsymbol{\pi}' \\ \sigma' \end{pmatrix} = \left[\mathbf{1}_{4 \times 4} + \sum_{i=1}^3 \theta_i^V V_i + \sum_{i=1}^3 \theta_i^A A_i \right] \begin{pmatrix} \boldsymbol{\pi} \\ \sigma \end{pmatrix}, \quad (3.22)$$

four-dimensional sphere since $\boldsymbol{\pi}$ and σ are subject to the constraint

$$\boldsymbol{\pi}^2 + \sigma^2 = F^2,$$

where F is a constant of dimension mass. Making use of this equation to eliminate σ in Eq. (3.22) we end up with the following transformation properties of $\boldsymbol{\pi}$ under $SO(4)$:

$$\begin{aligned} \boldsymbol{\pi} &\xrightarrow{\theta^V} \boldsymbol{\pi}' = \boldsymbol{\pi} + \boldsymbol{\theta}^V \times \boldsymbol{\pi}, \\ \boldsymbol{\pi} &\xrightarrow{\theta^A} \boldsymbol{\pi}' = \boldsymbol{\pi} + \boldsymbol{\theta}^A \sqrt{F^2 - \boldsymbol{\pi}^2}, \end{aligned} \quad (3.25)$$

where $\boldsymbol{\theta}^{V,A} \equiv \{\theta_i^{V,A}\}$ with $i = 1, 2, 3$. The nonlinear terms (in $\boldsymbol{\pi}$) on the right-hand side of the second equation give rise to the nonlinear realization of $SO(4)$. This is exactly what we wanted to achieve: the



As a last remark note that the four-dimensional rotations of $(\boldsymbol{\pi}, \sigma)$ can be conveniently written using the 2×2 matrix notation by introducing the unitary matrix²

$$U = \frac{1}{F} (\sigma \mathbf{1}_{2 \times 2} + i \boldsymbol{\pi} \cdot \boldsymbol{\tau}), \quad (3.26)$$

and demanding the transformation properties of U under chiral rotations to be:

$$U \longrightarrow U' = L U R^\dagger, \quad (3.27)$$

Here, L and R are $SU(2)_L \times SU(2)_R$ matrices defined in Eq. (3.18).

Towards an *ab initio* covariant density functional theory for nuclear structure

Shihang Shen^{a,b,c}, Haozhao Liang^{d,e}, Wen Hui Long^{f,g}, Jie Meng^{a,h,i,*}, Peter Ring^{a,j}

Prog. Part. Nucl. Phys. 109, 103713 (2019)

In the relativistic framework, the two-nucleon scattering equation is the Bethe-Salpeter equation

$$\mathcal{M} = \mathcal{V} + \mathcal{V} \mathcal{G} \mathcal{M},$$

where \mathcal{M} is the relativistic two-nucleon scattering amplitude and \mathcal{G} is the relativistic free two-nucleon propagator. In this equation, \mathcal{V} is the infinite sum of all irreducible diagrams and is usually replaced by the one-boson exchange contribution within the “ladder” approximation, $\mathcal{V} \approx V_{\text{OBE}}$ (the subscript “OBE” will be omitted without causing ambiguity).

three-dimensional reductions

$$\begin{aligned} \mathcal{M} &= \mathcal{W} + \mathcal{W} g \mathcal{M}, & \mathcal{W} &\approx V, & E_{\mathbf{q}}^2 &= M^2 + \mathbf{q}^2. \\ \mathcal{W} &= V + V(\mathcal{G} - g)\mathcal{W}, & \longrightarrow & \mathcal{M} = V + V g \mathcal{M}, \\ \text{a propagator } g &\text{ is introduced.} & \mathcal{M}(\mathbf{q}', \mathbf{q}|\mathbf{P}) &= V(\mathbf{q}', \mathbf{q}) + \int \frac{d^3k}{(2\pi)^3} V(\mathbf{q}', \mathbf{k}) \frac{M^2}{E_{\mathbf{k}} E_{\mathbf{P}/2+\mathbf{k}}} \frac{1}{2E_{\mathbf{q}} - 2E_{\mathbf{k}} + i\epsilon} \mathcal{M}(\mathbf{k}, \mathbf{q}|\mathbf{P}), \end{aligned}$$

$$\mathcal{M}(\mathbf{q}', \mathbf{q}|\mathbf{P}) = V(\mathbf{q}', \mathbf{q}) + \int \frac{d^3k}{(2\pi)^3} V(\mathbf{q}', \mathbf{k}) \frac{M^2}{E_{\mathbf{k}} E_{\mathbf{P}/2+\mathbf{k}}} \frac{1}{2E_{\mathbf{q}} - 2E_{\mathbf{k}} + i\epsilon} \mathcal{M}(\mathbf{k}, \mathbf{q}|\mathbf{P}),$$



$$\mathbf{P}=0$$

$$E_{\mathbf{q}}^2 = M^2 + \mathbf{q}^2.$$

$$T(\mathbf{p}', \mathbf{p}) = V(\mathbf{p}', \mathbf{p}) + \int \frac{d^3k}{(2\pi)^3} \frac{M^2}{\mathbf{k}^2 + M^2} \frac{V(\mathbf{p}', \mathbf{k}) T(\mathbf{k}, \mathbf{p})}{E - 2\sqrt{\mathbf{k}^2 + M^2} + i0^+},$$

Bethe-Salpeter equation

$$T(\vec{p}', \vec{p}) = V(\vec{p}', \vec{p}) + \int \frac{d^3p''}{(2\pi)^3} V(\vec{p}', \vec{p}'') \frac{M_N^2}{E_{p''}} \frac{1}{p^2 - p''^2 + i\epsilon} T(\vec{p}'', \vec{p})$$

$$E_{p''} \equiv \sqrt{M_N^2 + p''^2}.$$

Lippmann-Schwinger equation

$$\hat{T}(\vec{p}', \vec{p}) = \hat{V}(\vec{p}', \vec{p}) + \int d^3p'' \hat{V}(\vec{p}', \vec{p}'') \frac{M_N}{p^2 - p''^2 + i\epsilon} \hat{T}(\vec{p}'', \vec{p})$$